Thermal Characteristics of Discrete Heat Sources Using Coolants

Min-Goo Choi* and Keum-Nam Cho*

Key words : Multichip module, Paraffin slurry, Heat transfer coefficient, Cooling performance

Abstract

The present study investigated the effects of experimental parameters on the thermal characteristics of an in-line 6×1 array of discrete heat sources for a test multichip module using water, PF-5060 and paraffin slurry. The parameters were heat flux of 10-40W/cm², Reynolds number of 3,000~20,000 and mass fraction up to 10% for paraffin slurry. The size of paraffin slurry was within 10~40μm before and after experiments. The local heat transfer coefficients for the paraffin slurry were larger than those for water. Thermally fully developed conditions were observed after the third or fourth row (five or seven times of the chip length) and the paraffin slurry showed effective cooling performance at the high heat flux. The paraffin slurry with the mass fraction of 5% showed the most efficient cooling performance when the heat transfer and the pressure drop in the test section are considered simultaneously. The experimental data at the fourth and sixth rows are best agreed with the values predicted by the Malina and Sparrow's correlation among other correlations, and the empirical correlations for water and 5% paraffin slurry were obtained at the first and sixth rows when the channel Reynolds number is over 3,000.

Nomenclature

C_p : Specific heat at constant pressure [kJ/kgK]

D_h : Hydraulic diameters [m]

EF : Enhancement factor

f : Fanning friction factor, $\Delta P D_h / 2 \rho L U^2$

h : Heat transfer coefficient [W/m²K]

k : Thermal conductivity [W/mK]

L : Length [m]

Nu : Nusselt number, hD_h/k_f

ΔP : Pressure drop [Pa]

Pr : Prandtl number, $\mu_f C_p / k_f$

q'' : Heat flux [W/cm²]

* School of Mechanical Engineering, Sungkyunkwan University, Suwon 440-746, Korea

Re : Reynolds number, $\rho_f U D_h / \mu_f$
T : Temperature [℃]
U : Average velocity [m/s]
x : Mass fraction [%]

Greek letters

μ : Viscosity [Ns/m²]
ρ : Density [kg/m³]

Subscript

f : Working fluid
i : Inlet of the test section
s : Chip
sat : Saturation
sub : Subcooling

Superscript

+ : Dimensionless

1. Introduction

Continuing progress of complex and dense VLSI chips made the surface mounted technology (SMT) inefficient and have led to the development of a new packaging approach called multichip modules (MCM's). A MCM is defined as a packaging technique that places several semiconductor chips, interconnected with a high density substrate, into a single package. MCM's offer several advantages such as reduced weight, reduced size, increased reliability and enhanced performance. As the packaging density increases for a multichip module, an efficient cooling method is required. The heat flux should be removed within the ranges of 50~100W/㎠ for a single chip and up to 25W/㎠ for multichip module.[1-3] A direct liquid cooling method using fluorocarbon has been used for the cooling of multichip modules. Fluorocarbon is electrically insulating and chemically stable. The direct liquid cooling method using fluorocarbon is classified as the forced convection cooling[4-5], pool boiling cooling[6-7], forced convection boiling cooling.[8-9] But the direct liquid cooling has some problems such as maintenance and leaking problems of the electronic system and the thermal shock by thermal hysteresis which can occur at a chip. For these reasons, indirect liquid cooling is used in supercomputers recently (CRAY C916, C98 and C94). This requires the effective indirect liquid cooling method that can keep the surface temperature of the MCM's with high heat flux within the temperature limits.

Therefore, the present study is primarily concerned with measuring and comparing convective heat transfer data for a linear array of square heat sources with high heat flux playing the role of a MCM, cooled by indirect liquid cooling method using three kinds of coolants. And experimental results are compared with existing correlations for continuously heating condition, and correlations for discretely heating condition are provided.

2. Experimental apparatus and procedure

The schematic diagram of the experimental apparatus is shown in Fig. 1. The apparatus consisted of the test section, constant temperature bath, power supply, mass flow meter, pump, data acquisition system etc. The test section consisted of a rectangular channel and a multichip module. A rectangular channel with an aspect ratio of 0.2 shows the most efficient cooling performance for fully developed laminar single phase flow in case of top wall heating with uniform heat flux.[10] Since the

present study deals with fully developed turbulent flow and discrete heating of top wall, the result reported in the literature cannot directly apply to the present study.

Since no data on an aspect ratio were reported for fully developed turbulent flow, the aspect ratio of 0.2 (7.6 ± 0.05mm$\times 38.1 \pm 0.05$ mm) was chosen. The hydraulic diameter of the rectangular channel was 1.26cm.

The multichip module had an in-line 6×1 array of discrete heat sources simulated VLSI chips and it was flush mounted on the top wall of a horizontal acryl rectangular channel. The multichip module was located at 50 times of the hydraulic diameter from the inlet of the test section to make a hydrodynamically fully developed flow. A honeycomb was located at the inlet of the channel to make the flow uniform. Two static pressure taps connected to a U-tube manometer were located at the bottom wall to measure pressure drop. The heating wire with a resistance of $18.6 \pm 0.2\Omega$/m was attached on the simulated chip

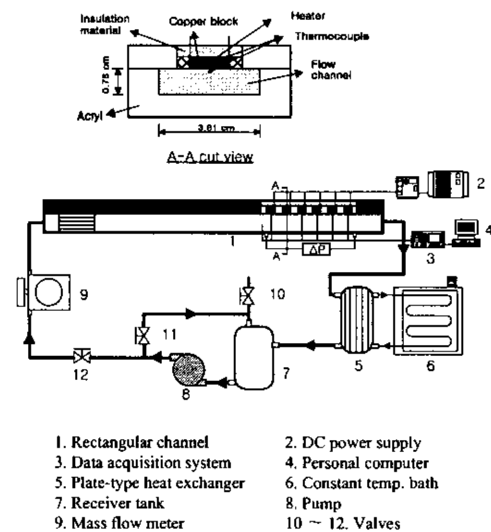

Fig. 1 Schematic diagram of the experimental apparatus.

by silicon glue for heating. Six heating wires on the chip were connected to the power supply with the accuracy of ± 0.03V in parallel to supply a uniform heat flux on each heater. Each heat source was the square with the size of 1.27cm which is the typical size for a VLSI chip. The distance between two close chips was 1.27cm. Copper heat sink with a thickness of 6mm was attached at the bottom of the chip and the other sides were thermally insulated by fiberglass to make the heat flow only to the channel. Copper heat sink was a square of the same size with the heater. The temperature difference on the copper heat sink with a thickness of 6mm was within the maximum of 0.5℃. The temperatures of the copper heat sink and the fluid temperatures just below (0.5mm) the copper heat sink surface were measured by type T thermocouples with the diameters of 0.127mm by inserting thermocouples in the machined holes. Thermocouples were calibrated within the accuracy of ± 0.15℃ by the standard RTD.

A conduction analysis was performed on the heat source and the substrate with thermal conductivities for the copper block (386 W/m · K), acryl (0.2W/m · K), thermal silicon (1.6W/m · K), and insulation (0.02W/m · K). The rate of heat loss from heater to ambient was 2.1~3.3% within whole experimental range and was compensated for heat flux value on heater.

The experiments were performed with water, PF-5060(a dielectric liquid manufactured by 3M Co.) and paraffin slurry. PF-5060 is an alternative coolant of FC-72, and its typical properties are shown and compared with FC-72 and water in Table 1.

Commercial grade paraffin which has the melting temperature of 43.5℃ and the fusion

Table 1 Properties of the Fluorinert liquids and water (at 25℃ and 1atm)

Property	PF-5060	FC-72	water
Boiling point (℃)	56	56	100
Density(Liquid) (g/cm^3)	1.68	1.68	1.0
Viscosity (cs)	0.4	0.4	0.9
Surface tension (dyne/cm)	12.0	12.0	72
Vapor pressure (kPa)	30	30	3.3
Heat of vaporization (cal/g)	21	21	540
Specific heat (cal/(g · ℃))	0.23	0.25	1.0

Table 2 Properties of Paraffin Waxes

Property		Value
Melting temperature (℃)		43.6
Heat of fusion (cal/g)		42.1
Specific heat (cal/g · ℃)	Liquid(at 60 ℃)	0.60
	Solid	0.71
Thermal conductivity (W/m · K)	Liquid(at 60 ℃)	0.17
	Solid	0.24
Density (g/cm^3)	Liquid(at 60 ℃)	0.76
	Solid	0.82
Viscosity (cP)(at 60 ℃)		3.14
Molecular weight (g/mol)		332

energy of 175.6kJ/kg measured by DSC (Differential Scanning Calorimetry) was used. Some thermal and physical properties of the paraffin are presented in Table 2. In order to make very fine paraffin particles, an emulsifier was used.

The experimental parameters were a the mass fraction of the paraffin slurry of 0, 2.5, 5, 7.5%, a heat flux of 10, 20, 30, and 40W/㎠ and a channel Reynolds number ranging from 3,000 to 20,000. The heat flux was obtained by dividing the heat amount supplied to each chip by the chip area and the Reynolds number is calculated by using the hydraulic diameter for the rectangular channel with an aspect ratio of 0.2. The inlet temperature of the test section was 15℃ for all runs.

The heat transfer coefficients were calculated by dividing the heat flux supplied by the chip by the temperature difference between the surface temperature of the chip and the fluid temperature 0.5mm below the chip. The error analysis of the heat transfer coefficients was conducted and the range was ±3.2~±3.8%.

3. Results and discussion

3.1 Size of the paraffin slurry particles

Paraffin slurry was made by cooling inside the bath which distilled water, liquid paraffin and emulsifier were mixed. In the mixture of water and paraffin, the two materials are immiscible, but if a small amount of emulsifier is injected to the mixture of water and paraffin, very fine particles are manufactured. The size of the paraffin particles must be small enough to prevent clogging in the flow loop. In the present study, optimal concentration of emulsifier to each mass fraction of paraffin was found by repetitive experiments and it was 3.3%. The size of the paraffin particles was 10~40㎛ and it was unchanged after the experiment as shown in Fig. 2. The density, specific heat, viscosity, and thermal conductivity of the paraffin slurry were obtained by equations which are reasonable on suspension and these were used at the data reduction process.

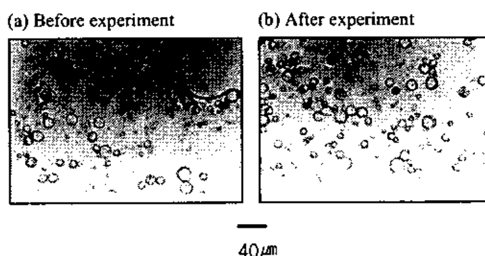

Fig. 2 Photographs of paraffin slurry with the mass fraction of 10%.

3.2 Pressure drop and friction factor in the test section

Figure 3 shows the pressure drop and apparent Fanning friction factor in the test section as a function of Reynolds number. Pressure drop is the difference between the static pressures at the inlet and outlet of the test section. The Blasius equation which can be used to predict the fully developed turbulent friction factor in smooth circular ducts was modified by Jones[11] to apply for rectangular ducts. The modified Blasius equation is defined as

$$f = 0.079\ (Re^{*}_{Dh})^{-0.25} \quad (1)$$

The Kozicki Reynolds number, Re^{*}_{DH}, in equation (1) is given by the following expression

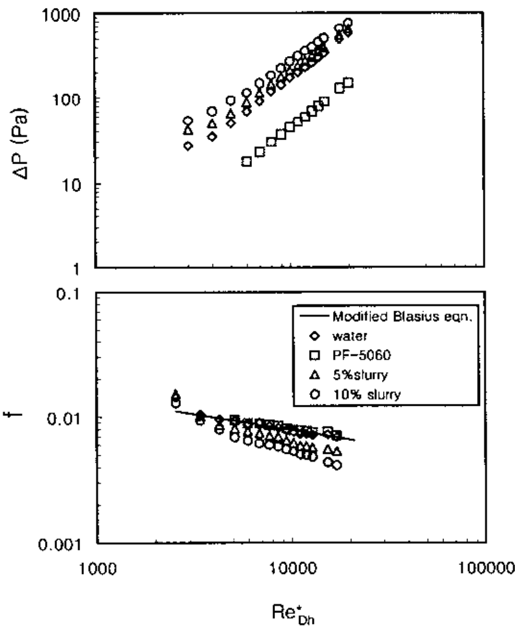

Fig. 3 Pressure drop and friction factor in the test section.

$$Re^{*}_{Dh} = a(\rho U D_h / \mu) \quad (2)$$

The a in equation (2) is a constant depending on the aspect ratio of rectangular channel. It is 0.85 when the aspect ratio of rectangular channel is 0.2.

The measured friction factors for water and PF-5060 at both 10 and 30W/㎠ were agreed within ±6% with the values predicted by the modified Blasius equation. As shown in Fig. 3, the pressure drop data for water were approximately 4 times larger than those for PF-5060, but the apparent Fanning friction factors for water and PF-5060 showed little difference. The reason is that pressure drop is proportional to the apparent Fanning friction factor and square of average velocity and the average velocity for water is about twice larger than that for PF-5060 at the same Reynolds number since the kinematic viscosity for water is 2.25 times larger than that for PF-5060 as shown in Table 1. The pressure drop data for the paraffin slurry were larger than those for water but the apparent Fanning friction factors for the paraffin slurry were smaller than those for water. The reason is that the average velocity for the paraffin slurry increases at the same Reynolds number since the kinematic viscosity for the paraffin slurry increases as the mass fraction of the paraffin slurry increases.

3.3 Chip surface temperature and boiling curve

The heat flux ranges for the chips are shown in Fig. 4 with respect to the chip surface temperatures at the first and sixth rows of multichip module when the channel Reynolds number is 20,000. For PF-5060 and water, the temperature difference

between the first and sixth rows increased as heat flux increases. The chip surface temperatures for water were lower than those for PF-5060 since the specific heat at constant pressure for PF-5060 is approximately 25% of that for water. As the heat flux increased to 30W/㎠, the boiling at the chip surface became more vigorous and the chip surface temperature differences between water and PF-5060 became smaller. But when heat flux is over 40W/㎠, the heater surface temperature for PF-5060 abruptly increases over 300℃ and the experiment couldn't be done.

The chip surface temperatures decreased as the mass fraction of paraffin slurry increased at the first and sixth rows and the decreasing rate of temperatures at high heat flux was larger than that at low heat flux. The chip surface temperatures for the paraffin slurry with the mass fraction of 5% were lower by about 11℃ than those for water at the heat flux of 40W/㎠. But the decreasing rate of the chip surface temperatures was not proportional to the mass fraction of paraffin slurry.

Boiling curve for PF-5060 is shown in Fig. 5 at the first and sixth rows for the average velocity at the inlet of test section of 0.386m/s (Re_{DH} =11,200) and a subcooling of 41℃. Subcooling (ΔT_{sub}) is a temperature difference between the saturation temperature of PF-5060 (T_{sat} =56℃) and inlet temperature (T_i =15℃). At low heat fluxes below approximately 5W/㎠, single phase convection is a dominant heat transfer mode even though the surface temperature is over the saturation temperature. The single phase convection effect at the first heater is larger than that at the sixth heater since the sixth heater is continuously affected by other heaters. The temperature overshoot was 3.5℃ and 2.6℃ at the

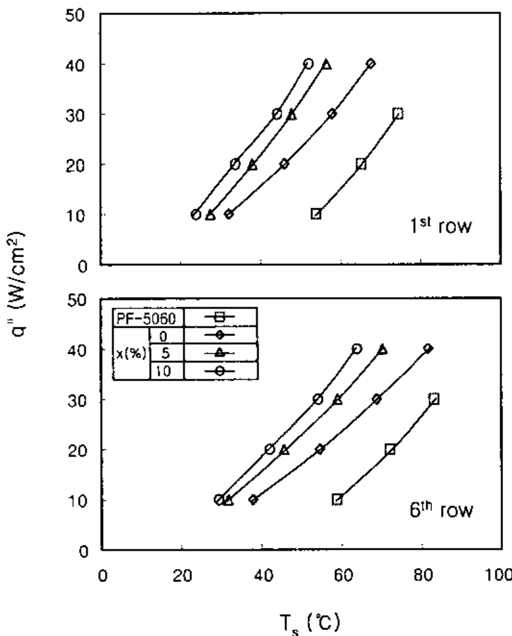

Fig. 4 Heat flux with respect to surface temperature (Re_{DH} =20,000).

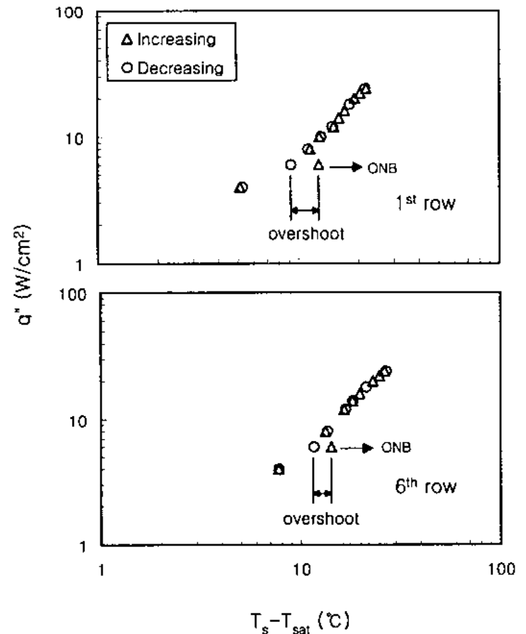

Fig. 5 Boiling curves for PF-5060 (U_i=0.386m/s, ΔT_{sub}=41℃).

first and sixth heaters. The temperature overshoot is defined as the difference of the temperature when the onset of nucleate boiling (ONB) is occurred and the temperature obtained from the boiling curve at the same heat flux with ONB.

3.4 Local heat transfer coefficients

The local heat transfer coefficients were obtained by using the chip surface temperature and fluid temperature just below the chip surface. Figure 6 shows the local heat transfer coefficients with respect to the row number when the channel Reynolds number is 20,000 and the heat flux is 10 and 30W/㎠. The local heat transfer coefficients reached to the uniform value approximately after the third or fourth row (five or seven times of the chip length). This means that it reached to a thermally fully developed condition after the

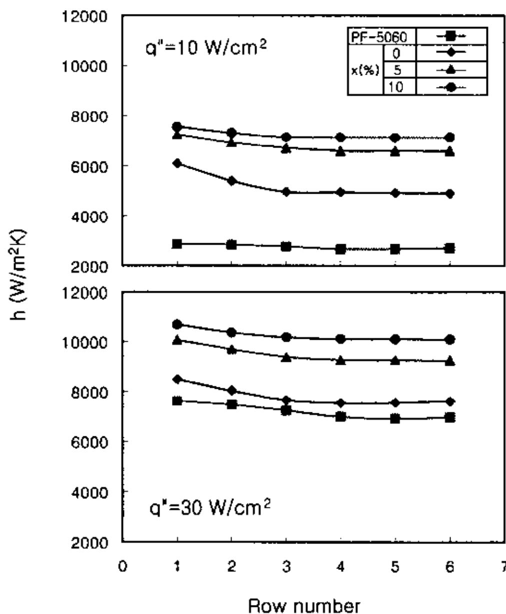

Fig. 6 Local heat transfer coefficient with respect to row number (Re_{DH} =20,000).

fourth row. The local heat transfer coefficients for water at the heat flux of 10W/㎠ were about 1.7~2.1 times larger than those for PF-5060. As the heat flux increased to 30W/㎠, the local heat transfer coefficients for water were larger by 5.5~11.2% than those for PF-5060. The reason is that as heat flux increases up to a certain value, subcooled nucleate boiling near heater surface makes local heat transfer coefficient for PF-5060 increase. The local heat transfer coefficients for the paraffin slurry were larger than those for water and PF-5060, which means that paraffin slurry shows more effective cooling performance than water. It is generally agreed that the heat transfer enhancements are the result of the particle migration and collision against wall in turbulent flow and the role of latent heat. Transverse migration of particles adjacent to a surface can aid in disrupting the laminar sublayer and increasing the heat transfer coefficient. And the latent heat of the PCM, which can be viewed as a form of specific heat, increases the heat transfer coefficient because the heat transfer coefficient increases as the one-third power of the specific heat for turbulent flow.

The enhancement factor (EF) obtained by using the local heat transfer coefficient and the pressure drop at the Reynolds number of 20,000 is shown in Fig. 7. EF is defined as

$$EF = \frac{h^+}{\Delta P^+} \tag{3}$$

where h+ and ΔP+ are the ratios of the local heat transfer coefficient and the pressure drop for paraffin slurry to those for water. Both for the heat flux of 10 and 40W/㎠, EF's of the paraffin slurry with the mass fraction of 5% showed the largest values. This means that the paraffin slurry with the mass frac-

tion of 5% shows the most effective cooling characteristics when the heat transfer and the pressure drop in the test-section are considered simultaneously.

The local Nusselt number is obtained by using the local heat transfer coefficients. The local Nusselt number data for water were compared with correlations by Sieder and Tate[12], Malina and Sparrow[13], Yakovlev[14] and Petukhov and Kirillov[15]. These correlations are on the fully developed turbulent forced convection in circular ducts for liquids with variable properties.

The comparison at the fourth and the sixth rows when the heat fluxes are 10 and 30W/㎠ is shown in Fig. 8. Even though the slopes of the experimental results are slightly lower than the Malina and Sparrow's correlation, the values predicted by the Malina and Sparrow's correlation are best agreed with the experimental data among correlations. For the heat flux of 10W/㎠, the local Nusselt numbers of the present study were lower by 2.2~7.6% than the values predicted by Malina and Sparrow's correlation, and for the heat flux of 30W/㎠, the Malina and Sparrow's correlation agreed with the experimental data with a maximum deviation of ±3%.

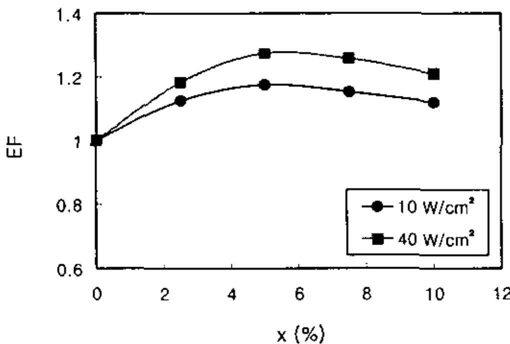

Fig. 7 Enhancement factor at the sixth row (Re_{DH} =20,000).

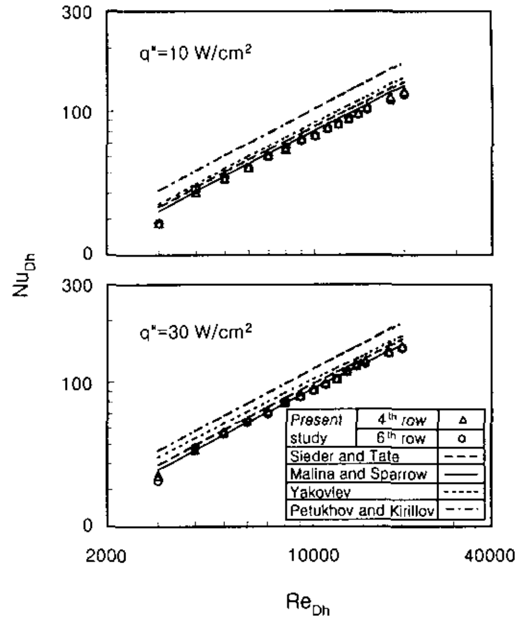

Fig. 8 Comparison of Nusselt number with the values predicted by various correlations for water.

For water and the paraffin slurry with the mass fraction of 5%, the Nusselt numbers at the first and sixth rows are shown in Fig. 9 with respect to the channel Reynolds number by using a viscosity ratio exponent of 0.05, and a Prandtl number exponent of 1/3. The Nusselt numbers for the first row are larger than those for the sixth row because the first row is in the thermally developing region. And the Nusselt numbers for the paraffin slurry with the mass fraction of 5% are larger by 9.7~27.8% than those for water at the heat flux of 30 W/㎠. The empirical correlations were obtained for water and the paraffin slurry with the mass fraction of 5% at the first and sixth rows when the channel Reynolds number is over 3,000. The correlations are of the form

$$\frac{Nu_{Dh}}{\Pr_f^{1/3}(\mu_f/\mu_s)^{0.05}} = C\ Re_{Dh}^m \quad (4)$$

where values of C and m are presented in Table 3.

4. Conclusions

The present study can be concluded as follows.

(1) The size of the paraffin slurry particles was 10~40㎛ and it was unchanged after the experiment.

(2) The measured friction factors for water and PF-5060 were agreed within ±6% with the values predicted by the modified Blasius equation and the apparent Fanning friction factors for the paraffin slurry were smaller than those for water.

(3) The chip surface temperatures for the paraffin slurry of 5% were lower than those for water and PF-5060. The temperatures for water were lower by 14.4~21.5℃ than those for PF-5060 at the heat flux of 30W/㎠, and from the boiling curve of PF-5060, the temperature overshoot was 3.5℃ and 2.6℃ at the first and sixth heaters.

(4) The local heat transfer coefficients for the paraffin slurry were larger than those for water due to the latent heat of paraffin slurry and the movements of paraffin slurry particles. The heat transfer coefficients reached to the uniform value approximately after the fourth row. This means that it reached to a thermally fully developed condition after the fourth row.

(5) The paraffin slurry with the mass fraction of 5% showed the most effective cooling characteristics when the heat transfer and the pressure drop in the test section are considered simultaneously.

(6) The values predicted by the Malina and Sparrow's correlation are best agreed with the experimental data, and the empirical correlations were obtained for water and 5% paraffin slurry at the first and sixth rows when the channel Reynolds number is over 3,000.

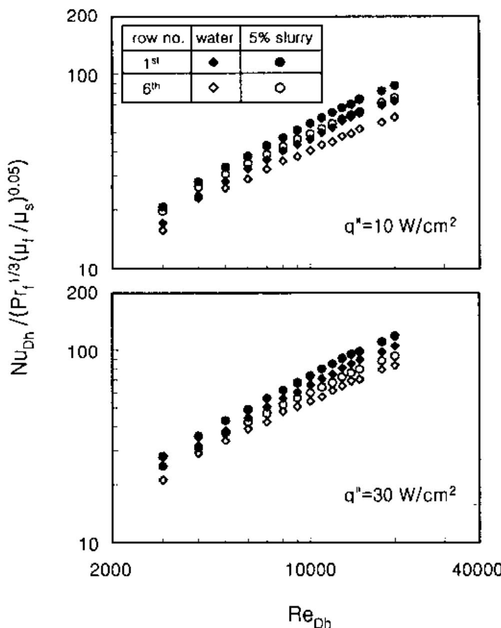

Fig. 9 Nusselt number with respect to Reynolds number for water and 5% paraffin slurry.

Table 3 Values of coefficient in equation (4)

Heat flux (W/cm²)	Mass fraction(%)	Row No.	C	m
10	0	1	0.083	0.692
		6	0.089	0.662
	5	1	0.057	0.746
		6	0.047	0.747
30	0	1	0.099	0.694
		6	0.086	0.698
	5	1	0.062	0.766
		6	0.059	0.760
Malina and Sparrow			0.023	0.8

Acknowledgments

The authors wish to acknowledge the financial support of the Korea Research Foundation(1998-018-E00018) in the program of 1998, and partly by the Brain Korea 21 project.

References

(1) Tummala, R. R., 1991, Electronic packaging in the 1990's - a perspective from america, IEEE Trans. Comp., Hybrids, Manuf. Technol., Vol. 14, No. 2, pp. 262-271.

(2) Ohsaki, T., 1991, Electronic packaging in the 1990's - a perspective form asia, IEEE Trans. Comp., Hybrids, Manuf. Technol., Vol. 14, No. 2, pp. 254-261.

(3) Hagge, J. K., 1992, State-of-the-art multichip modules for avionics, IEEE Trans. Comp., Hybrids, Manuf. Technol., Vol. 15, No. 1, pp. 29-41.

(4) Baker, E., 1972, Liquid cooling of microelectronic devices by free and forced convection, Microelectronics and Reliability, Vol. 11, pp. 213-222.

(5) Incropera, F. P., Kerby, J. S., Moffatt, D. F., Ramadhyani, S., 1986, Convection heat transfer from discrete heat sources in a rectangular channel, Int. J. Heat Mass Transfer, Vol. 29, pp. 1051-1058.

(6) Mudawar, I., Anderson, T. M., 1990, Parametric investigation into the effects of pressure, subcooling, surface augmentation and choice of coolant on pool boiling in the design of cooling systems for high power density electronic chips, ASME J. Electronic Packaging, Vol. 112, pp. 357-382.

(7) Park, K. A., Bergles, A. E., 1987, Natural convection heat transfer characteristics of simulated microelectronic chips, ASME J. Heat Transfer, Vol. 109, pp. 90-96.

(8) Heindel, T. J., Ramadhyani, S., Incropera, F. P., 1992, Liquid immersion cooling of a longitudinal array of discrete heat sources in protruding substrates: II-Forced convection boiling, ASME J. Electronic Packaging, Vol. 114, pp. 63-70.

(9) Mudawar, I., Maddox, D. E., 1990, Enhancement of critical heat flux from high power microelectronic heat sources in a flow channel, ASME J. Electronic Packaging, Vol. 112, pp. 241-248.

(10) Hartnett, J. P. Kostic, M., 1989, Heat transfer to Newtonian and non-Newtonian fluids in rectangular ducts, Advances in heat transfer, Vol. 19, pp. 247-356.

(11) Jones, Jr., O. C., 1976, An improvement in the calculation of turbulent friction in rectangular ducts, ASME Journal of Fluid Engineering, Vol. 98, pp. 173-181.

(12) Sieder, E. N. and Tate, G. E., 1936, Heat transfer and pressure drop of liquids in tubes, Ind. Eng. Chem., Vol. 28, pp. 1429-1453.

(13) Malina, J. A. and Sparrow, E. M., 1964, Variable property, constant property and entrance region heat transfer results for turbulent flow of water and oil in a circular tube, Chem. Eng. Sci., Vol. 19, pp. 953-962.

(14) Rogers, D. G., 1980, Forced convection heat transfer in single phase flow of a newtonian fluid in a circular pipe, CSIR Report CENG 322, Pretoria, South Africa.

(15) Petukhov, B. S., 1970, Heat transfer and friction in turbulent pipe flow with variable physical properties. Advances in Heat Transfer, Vol. 6, pp. 505-564.